On the significance of ultra-magnesian olivines in basaltic rocks

J.K. Keiding[1], R.B. Trumbull[1], I.V. Veksler[1,2], and D.A. Jerram[3]
[1]GFZ German Research Centre for Geosciences, Telegrafenberg, D-14473 Potsdam, Germany
[2]Technical University Berlin, Department of Mineralogy and Petrology, Ackerstrasse 71-76, D-13355 Berlin, Germany
[3]DougalEARTH Ltd., 12 Nevilles Cross Villas, Durham DH1 4JR, UK

ABSTRACT

Ultra-magnesian olivines in basaltic rocks or magma are here defined by a forsterite proportion [Fo = Mg/(Mg + Fe) in molar percent] greater than the maximum $Fo_{91.5}$ known from Earth's mid-ocean ridge systems. They are relatively common in Archean komatiites and have been also reported from several Phanerozoic large igneous provinces. The presence of ultra-magnesian olivines is generally interpreted as evidence for melts with extremely high MgO concentration (komatiites) and high eruption temperatures. Such melts are considered to be hallmarks of a hotter mantle in the early Earth and of thermal anomalies related to Phanerozoic mantle plumes. Here we show that the link between ultra-magnesian olivines and komatiitic melts is not straightforward. The composition of melt inclusions trapped in ultra-magnesian olivine ($Fo_{93.3}$) from the Etendeka province of Namibia contradict the predicted 24 wt% MgO for parental melts and 1680 °C mantle potential temperature. Instead, the trapped melts do not exceed 17.5 wt% MgO, and the maximum potential temperature indicated by these compositions is 1520 °C. We show that ultra-magnesian olivines can also be produced by protracted melt extraction from the mantle source, and that this process also leaves a distinctive depletion in incompatible trace elements.

INTRODUCTION

Constraining the original melt temperatures of basaltic rocks is an important step in understanding how variable mantle temperature is at present, and how it may have varied through Earth history. Arguably the best geothermometer for this is based on the Fe-Mg solid solution of olivine in equilibrium with basaltic melt, which follows well-established thermodynamic relationships among temperature, pressure, and phase composition. These relationships form the basis for comparative studies of melting temperatures for modern and ancient settings (mid-ocean ridge systems, oceanic islands, large igneous provinces [LIPs]; Green et al., 2001; Putirka, 2008; Putirka et al., 2007), and they are also used to estimate parental melt composition of more evolved basaltic suites.

The presence of ultra-magnesian olivines ($>Fo_{91.5}$) in komatiites is consistent with olivine-melt equilibrium relationships in these high-Mg rocks (by definition, >18 wt% MgO). Ultra-magnesian olivines in komatiites predominantly occur as phenocrysts, clearly distinguishable from those formed by crystal accumulations (Jerram et al., 2003). Komatiites are almost absent in the Phanerozoic record (the single known locality is Gorgona Island, Colombia), but ultra-magnesian olivines are not. They have been discovered in many Phanerozoic LIPs, i.e., Gorgona Island from the Caribbean oceanic plateau (Revillon et al., 2000), the Siberian Traps (Arndt et al., 1995), the North Atlantic LIP in West Greenland (Larsen and Pedersen, 2000) and Baffin Bay (Francis, 1985; Yaxley et al., 2004), the Emeishan LIP in southeast China and northern Vietnam (Hanski et al., 2010), the

Karoo LIP in Antarctica (Heinonen and Luttinen, 2010), and the Paraná-Etendeka LIP in northwest Namibia (Thompson and Gibson, 2000), the subject of this paper. Shared features of ultra-magnesian olivines in these provinces are that they are rare, occurring in just a few localities, and they are too Mg rich to be considered equilibrium phenocrysts in the basaltic host rocks. It is significant that these olivines coexist in the same hand specimens with much more abundant, less magnesian crystals (Fo_{85-90}), the compositions of which are close to equilibrium with the Mg# of the host rocks, and can therefore be considered as phenocrysts. It follows that the ultra-magnesian olivines are not phenocrysts in the present host, but represent xenocrysts. The high CaO contents in these olivines clearly distinguish them from entrained crystals of mantle olivine, and most studies have concluded that the ultra-magnesian crystals originated from an unerupted komatiitic melt and were incorporated into a second, more evolved magma. We emphasize that this conclusion is based only on olivine and bulk-rock compositions. However, olivine compositions constrain only the Mg# [MgO/(MgO + FeO) in molar percent] of the equilibrium liquid and not its MgO concentration, on which the inference of a komatiitic affinity and high temperature of the parental melts critically depend. To calculate the melt MgO requires information on its FeO content.

This study presents an example where original melt compositions are recovered directly by analysis of inclusions trapped in the ultra-magnesian olivines. This removes the dependence of the results on the bulk rock composition and provides a valuable test of the relationships of ultra-magnesian olivines to melt temperatures.

XENOCRYSTIC ORIGIN OF ULTRA-MAGNESIAN OLIVINES

We studied olivine-phyric dolerites from 22 dikes in the Henties Bay–Outjo dike swarm from the southern Etendeka Province of Namibia (Thompson et al., 2001; Trumbull et al., 2004, 2007). The samples are basaltic to picritic tholeiites (see Table DR1 in the GSA Data Repository[1]) with Mg# up to 79.4, they have a wide range of MgO contents (7.0–19.4 wt%), and olivine core compositions are characterized by highly variable forsterite contents ($Fo_{54.1-93.3}$; Table DR2). Ultra-magnesian olivines ($>Fo_{91.5}$) were found in four samples, including the one first described by Thompson and Gibson (2000), who interpreted these Mg-rich olivines to indicate nonerupted komatiitic melt. Most olivines with Fo >85 and all of the ultra-magnesian grains plot above the olivine-liquid equilibrium line for $K_D = 0.31$–0.35 (Fig. 1A), and we interpret them as entrained xenocrysts. This is supported by the range of olivine compositions in single samples (Fig. 1B) and by the presence of thin (5–10 μm) Fe-enriched rims (to Fo_{80}) on some grains due to reequilibration with the host magma. The bulk rock compositions in this case are clearly unsuited to investigate the melts from which the olivine crystallized. We prefer instead to use melt inclusions that are directly linked to the host olivines.

ULTRA-MAGNESIAN OLIVINE-HOSTED MELT INCLUSIONS

Melt inclusions range in size from 10 to 70 μm, are typically round, and are partly to completely crystalline, with daughter crystals of Al-rich clinopyroxene, Al-rich orthopyroxene, and spinel (chromite). Melt inclusions were heated to homogenization at 1350 °C before analysis of major and trace elements by electron microprobe and secondary ion mass spectrometry (see the methods section in the Data Repository). Measured compositions (Table DR3) were corrected for post-trapping crystallization on inclusion walls by incremental addition of equi-

---
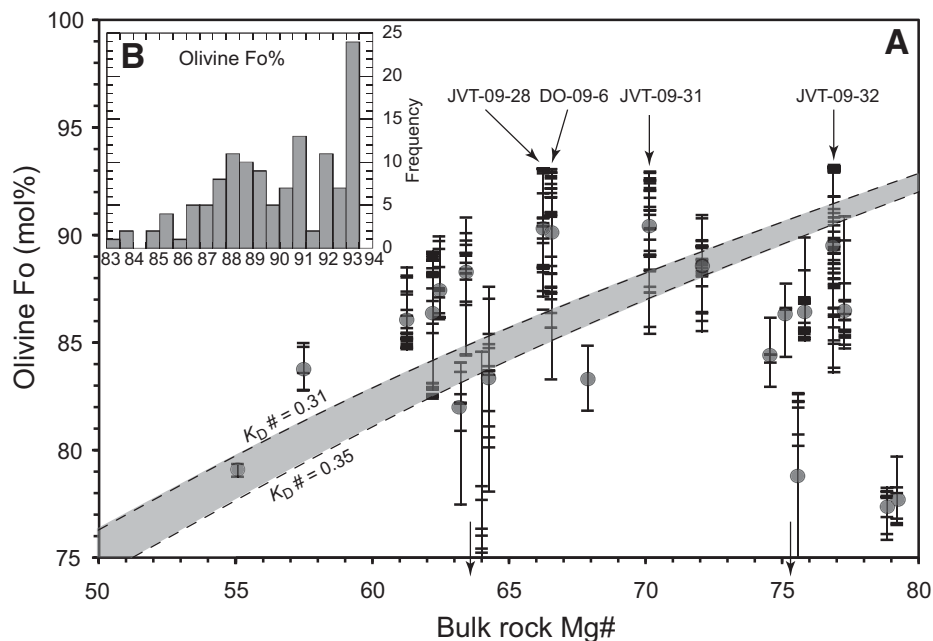
Figure 1. MgO-FeO relationship between olivines and rocks from Etendeka province (Namibia). A: Olivine forsterite content versus Mg# of rock containing them. Individual olivines are short horizontal bars; average olivine compositions are shown as circles. Dashed lines represent olivine melt equilibrium compositions for K_D = 0.31–0.35. Olivines plotting to left of dashed lines are interpreted as xenocrysts to rocks containing them, whereas olivines to right of lines are a result of olivine accumulation. Ultra-magnesian olivine samples studied here are indicated by arrows. B: Frequency histogram of olivine composition (Fo in mol%) from four samples indicated in A.

librium olivine (see the Data Repository). After correction, 58 of 66 homogenized inclusions yielded compositions consistent with Fe-Mg equilibrium with the olivine host, and these are considered reliable estimates of the entrapped melts (Table DR4; Fig. 2). A key feature of these compositions is the low FeO content compared with the bulk rocks, a vital clue to their origin, as described herein. We recognize that low FeO in melt inclusions can be an artifact caused by a post-entrapment process known as iron loss (Danyushevsky et al., 2000, 2002), whereby equilibration of inclusion walls with the bulk olivine drives inclusions toward lower FeO values and higher MgO than in the original melts (thus higher Mg#). Procedures to recognize and compensate for iron loss are well established, and we conclude that the low FeO contents of

melt inclusions in our study are not due to that process. The best evidence for this is that iron loss results in unreasonably high olivine-melt K_D values (>0.35), which are not observed for 90% of the inclusions reported here. Although the exceptional eight inclusions do yield high K_D values, compositional gradients in the olivine walls adjacent to them are the reverse of what iron loss would produce (Fig. DR1). We attribute the high K_D values of the eight outlier inclusions to unintentional overheating. Inclusions most affected by overheating are those with the lowest trapping temperatures and most evolved compositions, which are not of primary interest here.

POTENTIAL TEMPERATURE ESTIMATES

The 58 inclusions considered to represent equilibrium melts have 9.3–17.5 wt% MgO and Mg# values from 66.5 to 82.5 (Fig. 2; Table DR4). Olivine-melt equilibrium temperatures calculated for these compositions (following Putirka et al., 2007) range from 1246 °C to 1395 °C, with ultra-magnesian olivine and trapped melts at the upper end of this range. More useful than crystallization temperature for many purposes is the potential temperature of the mantle source, T_P, which expresses the mantle temperature projected along the solid-state adiabat to surface pressure. There are different ways to derive potential temperature (Herzberg et al., 2007; Herzberg and Gazel, 2009; Putirka, 2005; Putirka et al., 2007), and some require knowledge of variables that are difficult to accurately determine (e.g., degree of melting and pressure of melt formation). We use a simple relationship linking potential temperature in degrees Celsius with melt MgO concentration in weight percent (Herzberg et al., 2007; Herzberg and Gazel, 2009):

$$T_p = 1463 + 12.7 \, \text{MgO} - 2924 / \text{MgO}. \quad (1)$$

This formula allows one to calculate and compare T_P for any primary melt with a known MgO content. The maximum T_P for the Etendeka ultra-magnesian olivines and trapped melts calculated in this way is 1520 °C, which is within the range of values for Hawaii and Iceland (Herzberg et al., 2007; Herzberg and Gazel, 2009; Herzberg and O'Hara, 2002; Ribe and Christensen, 1999), but more than 150 °C lower than the 1680 °C inferred from an earlier study lacking melt inclusion data (Thompson and Gibson, 2000). Applying Equation 1 to the calculated melt of Thompson and Gibson (2000) results in a T_P of 1650 °C, which is still more than 100 °C higher than our estimate. We explain the higher temperatures estimated previously by the combination of bulk rock compositions with data from Mg-rich olivines that are xenocrysts in the rocks (Fig. 1). Instead of the
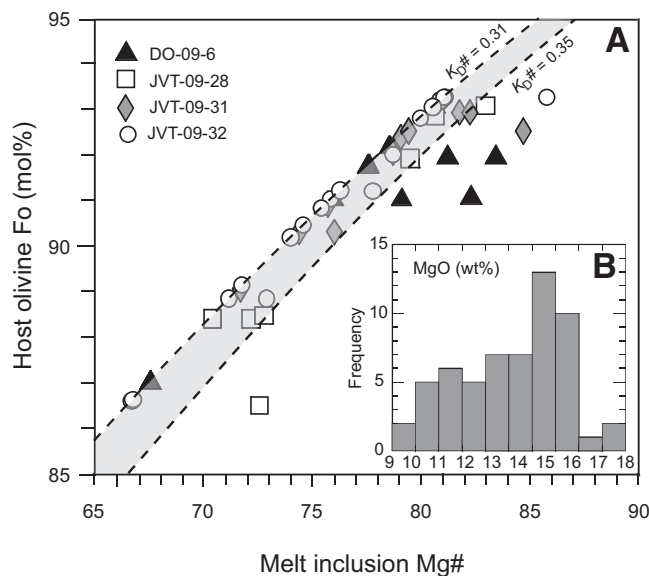
Figure 2. MgO-FeO relationship between melt inclusions and their host olivines. A: Mg-number of melt inclusions versus their host olivine compositions after correction for post-entrapment crystallization (see text). Dashed K_D lines as in Figure 1. Melt inclusions plotting to right of these lines are out of equilibrium with host olivine due to overheating during homogenization experiments (see the Data Repository and the methods section therein [see footnote 1]). B: Frequency histogram of MgO content in homogenized melt inclusions (wt%) after correction for post-entrapment crystallization.

predicted komatiitic melt with 24.0 wt% MgO (Thompson and Gibson, 2000, based on 11 wt% FeO), the observed melts actually have a maximum of 17.5 wt% MgO and ~7 wt% FeO. The important point is that both of these melt compositions can crystallize Fo_{93} olivines because they have the same Mg#. As pointed out by Herzberg and O'Hara (2002) and Herzberg et al. (2007), the process of dynamic or critical melting of the mantle can result in low melt FeO contents and high Mg#. The dynamic melting scenario envisions separation of small melt increments (1–2 vol%) from the source as it melts, leaving a successively more depleted residue in a rising mantle column (Elliott et al., 1991; Langmuir et al., 1977). This process offers an alternative explanation for ultra-magnesian olivines, and there is independent evidence for it in the minor and trace element composition of melt inclusions in the Etendeka olivines.

TRACE ELEMENT CHARACTERISTICS

Strong diversity of incompatible element abundances is a first-order feature of the Etendeka melt inclusions, both in single samples and individual crystals (Table DR4; Fig. 3). The lack of correlation between inclusion compositions and host forsterite content (Fig. 3) indicates that fractional crystallization did not control the observed melt diversity. Instead, we envisage a model where trapped melts are diverse because they are products of incremental melting and have not undergone mixing (Sobolev and Shimizu, 1993; Gurenko and Chaussidon, 1995). It is an accepted concept that basaltic magma represents an aggregate of melt increments generated by low-degree partial melting at the source and then mixed during ascent and storage. The value of melt inclusions is their ability to display these fine-scale features of melt variability that are lost in magmas that crystallize as bulk rocks.

The rare earth element (REE) concentrations of melt inclusions are especially illustrative of their diversity. Most inclusions have relatively flat REE patterns on a chondrite-normalized diagram, similar to those of the host dikes (Fig. 4). A second group of inclusions has steeper REE patterns, with enrichment in the light versus the medium REEs (e.g., La/Sm > 1). A third group of inclusions is characterized by low total REE abundance, and strong depletion of the light versus medium REEs (La/Sm < 1). The depleted melts show equally low relative concentrations of other highly incompatible elements like K, Ba, Th, and Nb (Fig. DR2). Similar, so-called ultra-depleted, inclusions have been found in olivine from the mid-Atlantic Ridge (Sobolev and Shimizu, 1993) and Iceland (Gurenko and Chaussidon, 1995; Slater et al., 2001), and in komatiite lavas from Gorgona Island (Arndt et al., 1997). Ultra-depleted compositions have been attributed to dynamic melting of the mantle,

and geochemical models of this process show good agreement with observed REE patterns in ours and other studies (Arndt et al., 1997; Elliott et al., 1991; Langmuir et al., 1977; Revillon et al., 2000). Ultra-depleted melts can also form by melting an already-depleted mantle source, but there is no evidence for strongly depleted mantle in the extensive literature on Etendeka dikes and lavas. The fact that single olivine crystals have trapped a range of melt compositions, only some of which are ultra-depleted, is consistent with a scenario of dynamic melting, with random trapping of variably mixed melt increments during olivine crystallization (Fig. 3).
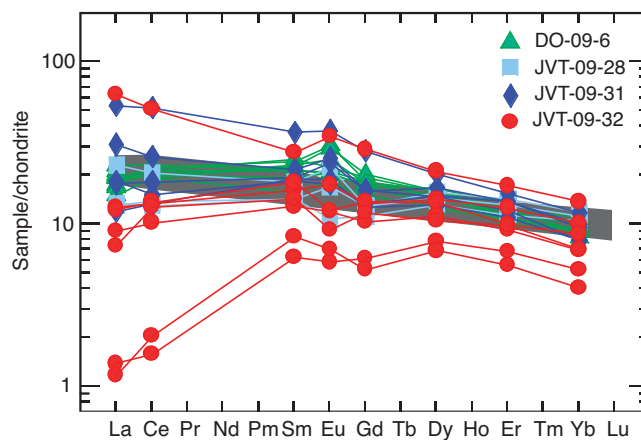
CONCLUSIONS

The main conclusion of this study is that ultra-magnesian olivines in basaltic rocks are not sufficient proof for high-temperature, komatiitic primary melts. The high Mg# in melts needed to crystallize Fo_{93} olivine can also result from Fe depletion of a mantle column undergoing dynamic melting. The melt inclusion data reported here suggest that Etendeka ultra-magnesian olivines formed in that way. Clearly, high-temperature, komatiitic primary melts will crystallize ultra-magnesian olivines. The komatiites of Gorgona Island are a case in point where erupted lavas match calculated parental melt compositions, and textural evidence indicates that the olivines are phenocrysts. However, for examples like the Etendeka and other Phanerozoic LIPs where komatiitic melts are inferred but not observed, and ultra-magnesian olivines may be xenocrysts, the dynamic melting scenario warrants careful consideration.
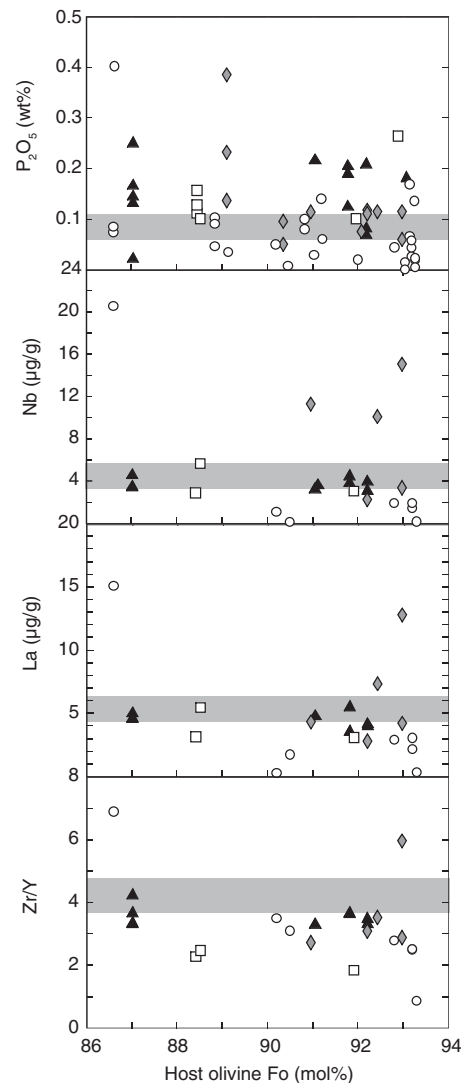
Figure 3. Selected element concentrations and ratios from melt inclusions plotted against host olivine compositions. Range of bulk rock compositions for these samples is shown as gray field for comparison. Symbols as in Figure 2.

Figure 4. Chondrite-normalized rare earth element patterns of studied melt inclusions. Bulk rock dike compositions for four samples are shown as gray field (data in Table DR5 [see footnote 1]). Normalizing factors are from Sun and McDonough (1989).

REFERENCES CITED

Arndt, N., Lehnert, K., and Vasilev, Y., 1995, Meimechites: Highly magnesian lithosphere-contaminated alkaline magmas from deep subcontinental mantle: Lithos, v. 34, p. 41–59, doi:10.1016/0024-4937(94)00032-W.

Arndt, N.T., Kerr, A.C., and Tarney, J., 1997, Dynamic melting in plume heads: The formation of Gorgona komatiites and basalts: Earth and Planetary Science Letters, v. 146, p. 289–301, doi:10.1016/S0012-821X(96)00219-1.

Danyushevsky, L.V., Della-Pasqua, F.N., and Sokolov, S., 2000, Re-equilibration of melt inclusions trapped by magnesian olivine phenocrysts from subduction-related magmas: Petrological implications: Contributions to Mineralogy and Petrology, v. 138, p. 68–83, doi:10.1007/PL00007664.

Danyushevsky, L.V., Sokolov, S., and Falloon, T.J., 2002, Melt inclusions in olivine phenocrysts: Using diffusive re-equilibration to determine the cooling history of a crystal, with implications for the origin of olivine-phyric volcanic rocks: Journal of Petrology, v. 43, p. 1651–1671, doi:10.1093/petrology/43.9.1651.

Elliott, T.R., Hawkesworth, C.J., and Grönvold, K., 1991, Dynamic melting of the Iceland plume: Nature, v. 351, p. 201–206, doi:10.1038/351201a0.

Francis, D., 1985, The Baffin Bay lavas and the value of picrites as analogues of primary magmas: Contributions to Mineralogy and Petrology, v. 89, p. 144–154, doi:10.1007/BF00379449.

Green, D.H., Falloon, T.J., Eggins, S.M., and Yaxley, G.M., 2001, Primary magmas and mantle temperatures: European Journal of Mineralogy, v. 13, p. 437–451, doi:10.1127/0935-1221/2001/0013-0437.

Gurenko, A.A., and Chaussidon, M., 1995, Enriched and depleted primitive melts included in olivine from Icelandic tholeiites: Origin by continuous melting of a single mantle column: Geochimica et Cosmochimica Acta, v. 59, p. 2905–2917, doi:10.1016/0016-7037(95)00184-0.

Hanski, E., Kamenetsky, V.S., Luo, Z.-Y., Xu, Y.-G., and Kuzmin, D.V., 2010, Primitive magmas in the Emeishan Large Igneous Province, southwestern China and northern Vietnam: Lithos, v. 119, p. 75–90, doi:10.1016/j.lithos.2010.04.008.

Heinonen, J.S., and Luttinen, A.V., 2010, Mineral chemical evidence for extremely magnesian subalkaline melts from the Antarctic extension of the Karoo large igneous province: Mineralogy and Petrology, v. 99, p. 201–217, doi:10.1007/s00710-010-0115-9.

Herzberg, C., and Gazel, E., 2009, Petrological evidence for secular cooling in mantle plumes: Nature, v. 458, p. 619–622, doi:10.1038/nature07857.

Herzberg, C., and O'Hara, M.J., 2002, Plume-associated ultramafic magmas of Phanerozoic age: Journal of Petrology, v. 43, p. 1857–1883, doi:10.1093/petrology/43.10.1857.

Herzberg, C., Asimow, P.D., Arndt, N., Niu, Y.L., Lesher, C.M., Fitton, J.G., Cheadle, M.J., and Saunders, A.D., 2007, Temperatures in ambient mantle and plumes: Constraints from basalts, picrites, and komatiites: Geochemistry Geophysics Geosystems, v. 8, p. 34, doi:10.1029/2006GC001390.

Jerram, D.A., Cheadle, M.J., and Philpotts, A.R., 2003, Quantifying the building blocks of igneous rocks: Are clustered crystal frameworks the foundation?: Journal of Petrology, v. 44, p. 2033–2051, doi:10.1093/petrology/egg069.

Langmuir, C.H., Bender, J.F., Bence, A.E., and Hanson, G.N., 1977, Petrogenesis of basalts from the FAMOUS area: Mid-Atlantic Ridge: Earth and Planetary Science Letters, v. 36, p. 133–156, doi:10.1016/0012-821X(77)90194-7.

Larsen, L.M., and Pedersen, A.K., 2000, Processes in high-Mg, high-T magmas: Evidence from olivine, chromite and glass in Palaeogene picrites from West Greenland: Journal of Petrology, v. 41, p. 1071–1098, doi:10.1093/petrology/41.7.1071.

Putirka, K.D., 2005, Mantle potential temperatures at Hawaii, Iceland, and the mid-ocean ridge system, as inferred from olivine phenocrysts: Evidence for thermally driven mantle plumes: Geochemistry Geophysics Geosystems, v. 6, p. 14, doi:10.1029/2005GC000915.

Putirka, K., 2008, Excess temperatures at ocean islands: Implications for mantle layering and convection: Geology, v. 36, p. 283–286, doi:10.1130/G24615A.1.

Putirka, K.D., Perfit, M., Ryerson, F.J., and Jackson, M.G., 2007, Ambient and excess mantle temperatures, olivine thermometry, and active vs. passive upwelling: Chemical Geology, v. 241, p. 177–206, doi:10.1016/j.chemgeo.2007.01.014.

Revillon, S., Arndt, N.T., Chauvel, C., and Hallot, E., 2000, Geochemical study of ultramafic volcanic and plutonic rocks from Gorgona Island, Colombia: The plumbing system of an oceanic plateau: Journal of Petrology, v. 41, p. 1127–1153, doi:10.1093/petrology/41.7.1127.

Ribe, N.M., and Christensen, U.R., 1999, The dynamical origin of Hawaiian volcanism: Earth and Planetary Science Letters, v. 171, p. 517–531, doi:10.1016/S0012-821X(99)00179-X.

Slater, L., McKenzie, D., Gronvold, K., and Shimizu, N., 2001, Melt generation and movement beneath Theistareykir, NE Iceland: Journal of Petrology, v. 42, p. 321–354, doi:10.1093/petrology/42.2.321.

Sobolev, A.V., and Shimizu, N., 1993, Ultra-depleted primary melt included in an olivine from the Mid-Atlantic Ridge: Nature, v. 363, p. 151–154, doi:10.1038/363151a0.

Sun, S.-s., and McDonough, W.F., 1989, Chemical and isotopic systematics of oceanic basalts: Implications for mantle composition and processes, in Saunders, A.D., and Norry, A.D., eds., Magmatism in the ocean basins: Geological Society of London Special Publication 42, p. 313–345, doi:10.1144/GSL.SP.1989.042.01.19.

Thompson, R.N., and Gibson, S.A., 2000, Transient high temperatures in mantle plume heads inferred from magnesian olivines in Phanerozoic picrites: Nature, v. 407, p. 502–506, doi:10.1038/35035058.

Thompson, R.N., Gibson, S.A., Dickin, A.P., and Smith, P.M., 2001, Early Cretaceous basalt and picrite dykes of the southern Etendeka region, NW Namibia: Windows into the role of the Tristan mantle plume in Parana-Etendeka magmatism: Journal of Petrology, v. 42, p. 2049–2081, doi:10.1093/petrology/42.11.2049.

Trumbull, R.B., Vietor, T., Hahne, K., Wackerle, R., and Ledru, P., 2004, Aeromagnetic mapping and reconnaissance geochemistry of the Early Cretaceous Henties Bay–Outjo dike swarm, Etendeka Igneous Province, Namibia: Journal of African Earth Sciences, v. 40, p. 17–29, doi:10.1016/j.jafrearsci.2004.07.006.

Trumbull, R.B., Reid, D.L., de Beer, C., van Acken, D., and Romer, R.L., 2007, Magmatism and continental breakup at the west margin of southern Africa: A geochemical comparison of dolerite dikes from northwestern Namibia and the Western Cape: South African Journal of Geology, v. 110, p. 477–502, doi:10.2113/gssajg.110.2-3.477.

Yaxley, G.M., Kamenetsky, V.S., Kamenetsky, M., Norman, M.D., and Francis, D., 2004, Origins of compositional heterogeneity in olivine-hosted melt inclusions from the Baffin Island picrites: Contributions to Mineralogy and Petrology, v. 148, p. 426–442, doi:10.1007/s00410-004-0613-z.